

## Physiological Parameters for Skin Rendering Using Spectrophotometer

Seonghyeon Moon<sup>1</sup>, Seonghee Lee<sup>2</sup> and Seongah Chin<sup>3</sup>

*Division of Multimedia, College of Engineering, Sungkyul University,  
Anyang, South Korea*

<sup>1</sup>*msh365@naver.com*, <sup>2</sup>*sunghi014@gmail.com*,  
<sup>3</sup>*solideo@sungkyul.edu*, corresponding author

### **Abstract**

*In this study, we apply skin data extracted from a spectrophotometer to a rendering model. We first divide the skin layers into the epidermis and dermis layers and then obtain the absorption and scattering coefficients for the wavelengths that match each skin layer. The absorption coefficient for each wavelength reflects the hemoglobin and melanin levels. Then, we store the percentage values of the hemoglobin and melanin levels as a table in a database and find from the database the hemoglobin and melanin levels closest to the skin color of a person, as obtained with a spectrophotometer.*

**Keywords:** *Spectrophotometer, Wavelength, Reflectance, Melanin, Hemoglobin*

### **1. Introduction**

In a modern society where many people are preoccupied with enhancing their appearance, the interest in skin is very high. The overall color of a skin varies according to the amount of melanin pigment and blood in the skin; this amount is affected by hereditary factors and is dependent on the biological race as well as the individual's constitution even within the same race.

The melanin level varies depending on non-hereditary factors as well. The changes in melanin cells can be one of the causes of skin aging: when the skin is exposed to a considerable amount of sunlight, the number of melanin cells increases in order to protect the skin from ultraviolet (UV) rays. Meanwhile, if the skin has not been sufficiently exposed to sunlight, the number of melanin cells decreases as a result of skin aging. Our previous research has been published about rendering with GPU program using BRDF model that reflects the microscopic roughness of the skin [12].

The skin color also changes depending on the flow of blood [13]. For example, while the belly, chest, etc. show the original skin color, the palm appears reddish because several blood capillaries run right below the skin of the palm. In short, the skin shows a sensitive and noticeable change depending on the amount of melanin and blood. In this study, we extract the melanin and hemoglobin levels in the individual's skin by using a spectrophotometer. The main objective of this study is to perform a custom skin component analysis on each individual's skin and to visualize the changes in skin color according to the skin ingredients by applying the extracted parameters to the rendering equations. To extract the accurate hemoglobin and melanin levels of real human skin, we apply the levels found from the database to the BSSRDF rendering model developed by Wang [10] and seven other

researchers and to the proposed model constructed with the BSSRDF equation formulated by Jensen [4], and compare them with actual skin data

## 2. Skin Structure and Light Characteristics

The physical structure and the chemical characteristics of skin are well-researched topics in various scientific fields. In this study, we use a two-layer skin model composed of the dermis and epidermis layers, which is suitable for subsurface scattering modeling.

### 2.1. Skin layers

The skin has a multi-layered structure. There are several different skin layers and a significant amount of research has been conducted on these; however, for the purpose of this study, we divide the skin into two main layers in order to extract the parameters required for the rendering equations. The outmost layer of the skin is the stratum corneum, which can be ignored in the considered model as it is so thin that the penetrating light is mostly scattered and barely absorbed by it. The epidermis layer is right beneath the stratum corneum, and most of the melanin cells are located in this layer. A melanin cell has color information and can be divided into the eumelanin and the pheomelanin. With respect to the wide variety of skin colors, the eumelanin emits a color from brown to black and the pheomelanin, a color from yellow to red. The dermis is the bottom layer of the skin where blood flows. The color of blood is due to hemoglobin, which can be classified as oxygenated hemoglobin and deoxygenated hemoglobin. In the next section, we describe the spectral equations for the epidermis and the dermis layers.

### 2.2. Absorption coefficient

The following equation is used for computing the absorption coefficients of the pheomelanin [2] and the eumelanin [1] in the epidermis layer [6].

$$\sigma_a^{pm}(\lambda) = 2.9 \times 10^{14} \times \lambda^{-4.75} mm^{-1} \quad (1)$$

$$\sigma_a^{em}(\lambda) = 6.6 \times 10^{10} \times \lambda^{-3.33} mm^{-1} \quad (2)$$

The two equations given above describe the spectral melanin absorption coefficients, where  $\lambda$  represents the wavelength of light and  $\sigma_a^{pm}$  and  $\sigma_a^{em}$  denote the spectral absorption coefficients of the pheomelanin and the eumelanin, respectively. A baseline model containing the basic elements of skin shows the spectral absorption coefficients of all the skin elements except organelles, cell membranes, fibrils, and melanin [3, 6, 14].

$$\sigma_a^{base}(\lambda) = 0.0244 + 8.53e^{-(\lambda-154)/66.2} mm^{-1} \quad (3)$$

The following equation is for the epidermis layer derived from the melanin and the baseline equations [7].

$$\sigma_a^{epi}(\lambda) = (C_m) \left( B_m \sigma_a^{em}(\lambda) + (1 - B_m) \sigma_a^{pm}(\lambda) \right) + (1 - C_m) \sigma_a^{base}(\lambda) \quad (4)$$

$C_m$  denotes the total volume fraction of melanin in the epidermis layer, and  $B_m$  adjusts the amount of eumelanin with respect to pheomelanin and exhibits a light tan or yellowish

appearance. If the value of  $B_m$  gets closer to 1, the amount of pheomelanin increases accordingly, emitting a brown or black color.

The dermal layer is close to the deeper areas of skin where the vascular capillary network carries blood. Hemoglobin exists in an oxygenated or deoxygenated state within the dermis. As the spectral absorption coefficients of hemoglobin have been clinically studied, we can apply them to the following equation in order to obtain the absorption coefficient in the dermis layer [6, 7]. Figure 1 shows an example.

$$\sigma_a^{der}(\lambda) = C_h (\gamma \sigma_a^{oxy}(\lambda) + (1 - \gamma) \sigma_a^{deoxy}(\lambda)) + (1 - C_h) \sigma_a^{baseline}(\lambda) \quad (5)$$

$C_h$  denotes the hemoglobin concentration in the dermis, and  $\gamma$  represents the ratio between the oxygenated and the deoxygenated hemoglobin.  $\gamma$  varies only slightly over different skin types and body locations by approximately 0.6–0.8. In our model, we set  $\gamma = 0.75$  [7, 9].

**Table 1. Parameters to Craig Donner model**

Parameter	Description	Range
$C_h$	Hemoglobin fraction	0.001-0.1
$C_m$	Melanin fraction	0-0.5
$B_m$	Melanin-type blend	0-1

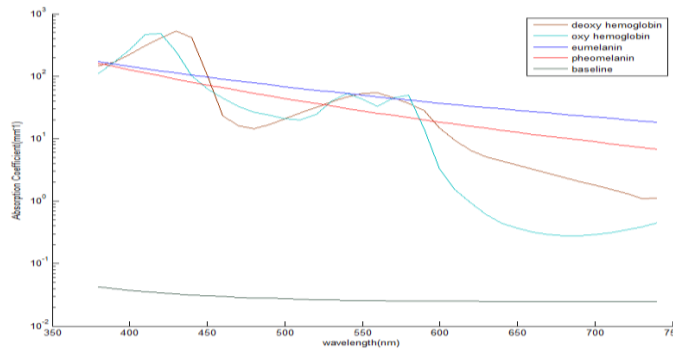


**Figure 1. Absorption coefficients of different skin elements for wavelengths between 380 and 740 nm**

### 2.3 Scattering coefficient

Light scattering in skin produces many small elements, such as the vessel wall, collagen, and fibril. The following approximated equation describes the reduced scattering in skin [7, 10].

$$\sigma_s' = 14.74\lambda^{-0.22} + 2.2 \times 10^{11} \times \lambda^{-4} \quad (6)$$

Eq. (6) is derived by combining Mie and Rayleigh's scattering equations. In general, a scattering equation is based on the assumption that the amount of light scattering is identical in all layers. However, Eq. (6) scales the reduced scattering coefficient by 50% in the dermis layer when the index of relative refraction is 1.4. Figure 2 shows scattering coefficients for wavelengths.

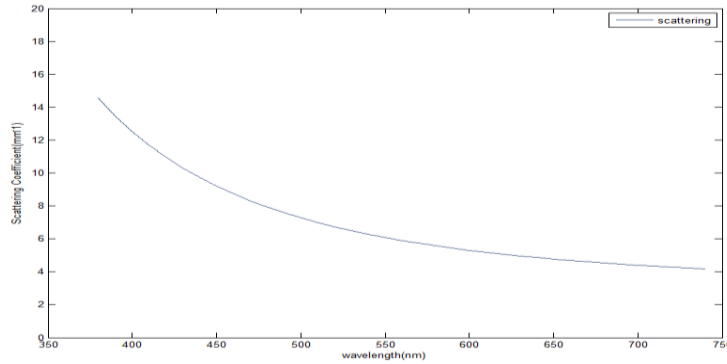


**Figure 2. Scattering coefficients for wavelengths between 380 and 740 nm**

We apply the above equations to the dipole model [4] developed by Henrik Jenson and the BSSRDF rendering model [10] developed by Rui Wang *et al.*, and create a database of the hemoglobin and melanin levels by different wavelengths.

### 3. Skin data extraction by spectrophotometer

A spectrophotometer is used for measuring the reflectance of an object. There are two methods for measuring reflectance: one is SCI representing reflection that includes the specular light reflection, and the other is SCE representing reflection that excludes it. Further, the measured color values in the L \* a \* b color space can be converted into other color spaces such as RGB and XYZ. In this study, we will use an SCE value that excludes the specular light reflection.

#### 3.1. Finding skin data using spectrophotometer

The spectral SCE reflection value measured with a spectrophotometer excludes the specular light reflection and is the final output from the diffusion approximation dipole model suggested by Jenson. Accordingly, we need to find the melanin and hemoglobin levels closest to the diffused color of the observed skin. Therefore, we use a spectrophotometer to collect the melanin and hemoglobin levels from various skin samples, translate them into RGB values, and store the translated values in a database. This database can be referenced to find out the closest RGB record from a given RGB input. Once the best-matching RGB record is found, we can extract the  $C_m$ ,  $B_m$  and  $C_h$  values and determine the melanin and hemoglobin levels of the skin.

#### 3.2. Comparison upon application to skin color

The parameters used for Figure 3 are  $\sigma_a$  and  $\sigma'_s$ . The spectral absorption and reduced scattering coefficients from Eqs. (4), (5), and (6) are converted into an XYZ value to show a color and then further converted into an RGB value. In order to optimized R channel we added some weights to G channel. With the computed spectral RGB values for  $\sigma_a$  and  $\sigma'_s$  we perform rendering on the basis of the dipole model equation formulated by Jenson, and test whether  $C_m$ ,  $B_m$ , and  $C_h$  capture the characteristics of melanin and hemoglobin.

## 4. Experimental Result

To verify  $\sigma_a$  and  $\sigma'_s$ , we performed a rendering simulation. As rendering equations, we used the diffusion approximation based on the dipole model by Jensen and the BRDF approximation [4]. We experimented on a platform with Intel® Core™ i7-3770 CPU and NVIDIA GeForce GTX 680, and used OpenGL and Cg Shader as the graphic and shading languages.

### 4.1. Diffusion approximation

Diffusion approximation is suitable for rendering a medium with a high scattering coefficient, which is a function/equation of  $\sigma_a$  (absorption coefficient),  $\sigma'_s$  (reduced scattering coefficient), and  $\eta$  (Fresnel coefficient). Diffusion reflectance can be computed as follows:

$$R_d(\|x_o - x_i\|) = \frac{\mu'}{4\pi} \left[ (\sigma_{tr} d_r + 1) \frac{e^{-\sigma_{tr} d_r}}{\sigma'_t d_r^3} + z_v (\sigma_{tr} d_v + 1) \frac{e^{-\sigma_{tr} d_v}}{\sigma'_t d_v^3} \right] \quad (7)$$

where  $\|x_o - x_i\|$  denotes the distance from the incident point to the outlet;  $\mu' = \sigma'_s / \sigma'_t$  the reduced albedo;  $\mu' = \sigma'_s / \sigma'_t$ , the reduced extinction coefficient;  $\sigma_{tr} = \sqrt{3\sigma_a \sigma'_t}$ , the effective transport extinction coefficient;  $d_r = \sqrt{z_r^2 + r^2}$ , the distance to the real light source;  $d_v = \sqrt{z_v^2 + r^2}$  is the distance to the virtual source.  $z_r = 1/\sigma_t$  and  $z_v = z_r + 4AD$  represent the distance from the dipole lights to the surface. Further, the A and D values in  $z_v$  can be calculated using the following equation:

$$A = \frac{1+F_{dr}}{1-F_{dr}}, \quad D = \frac{1}{3\sigma'_t} \quad (8)$$

where  $F_{dr} = \left( \frac{-1.44}{\eta^2} + \frac{0.71}{\eta} + 0.668 + 0.0636\eta \right)$  with the Fresnel reflex index  $\eta$ . In our experiments, we use 1.4, which is the most common value of this index with respect to the skin reflex. To implement Eq. (7) in the shading code, we need to transform each term in the equation solely as a function of  $\sigma_a$  and  $\sigma'_s$ , which are the input values to Eq. (7). First, if we transform the  $\sigma'_t$  terms with  $\sigma'_s + \sigma_a$ , we obtain  $\mu' = \frac{\sigma'_s}{\sigma'_s + \sigma_a}$ ,  $\sigma_{tr} = \sqrt{3\sigma_a(\sigma'_s + \sigma_a)}$ ,  $z_r = \frac{1}{\sigma'_s + \sigma_a}$ , and  $D = \frac{1}{3(\sigma'_s + \sigma_a)}$ .

Moreover, if we apply the transformed  $z_r$  to the remaining terms, we obtain the following:

$$d_r = \sqrt{\left( \frac{1}{\sigma'_s + \sigma_a} \right)^2 + r^2}, \quad z_v = \frac{1}{\sigma'_s + \sigma_a} + 4A(3\sigma'_s + 3\sigma_a), \quad d_v = \sqrt{\left( \frac{1}{\sigma'_s + \sigma_a} + 4A(3\sigma'_s + 3\sigma_a) \right)^2 + r^2}$$

### 4.2 BRDF approximation

BRDF approximation is applied for obtaining the total diffuse reflectance by integrating BSSRDF over the surface. After integrating Eq. (7), we obtain the following:

$$R = 2\pi \int_0^\infty R_d(r) r dr = \frac{\mu'}{2} \left( 1 + e^{-\frac{4}{3}A\sqrt{3(1-\mu')}} \right) e^{-\sqrt{3(1-\mu')}} \quad (9)$$

where  $r = \|x_o - x_i\|$  denotes the distance from the incident point to the outlet. However, the integration effectively adds up  $R_d$  for every distance  $r$ , and we do not need  $r$  in the BRDF approximation. Moreover, we can compute  $\mu'$  using  $\sigma_a$  and  $\sigma'_s$ , as mentioned earlier.

Therefore, we can experimentally verify the BRDF approximation with the parameters computed thus far.

### 4.3. Diffusion rendering

The requirement in BSSRDF with respect to shading is that for computing the color of a point on an object, we should consider the light interaction with all the points around this point. When we apply this concept to Eq. (7), we observe that the range of such an interaction is  $\|x_o - x_i\|$ , which is the distance from the incident point to the outlet. Therefore, we can obtain the color of a point of interest ( $x_o$ ) by computing many  $R_d$  values based on the distance from  $x_o$  to all the adjacent points ( $x_i$ ) and summing up all these values.

However, this approach to obtaining the color of a certain point can be too expensive to accomplish in real-time rendering as it requires us to sample all the points in an object and compute the  $R_d$  values for all of them. Hence, PCA-based rendering [10] and sampling and rendering in an image space have been proposed for real-time rendering. These schemes use pre-computed/stored data instead of pixel information in order to speed up the 2D texture rendering.

However, we devised a simpler way of computing  $R_d$  by replacing  $\|x_o - x_i\|$  in Eq. (7) with the distance from the (x, y) coordinate under the light to the (x, y) coordinate where we like to compute the color on the viewpoint. By repeating the same process multiple times, we found each  $R_d$  value and added the specula to the result, leading to Figure 3.

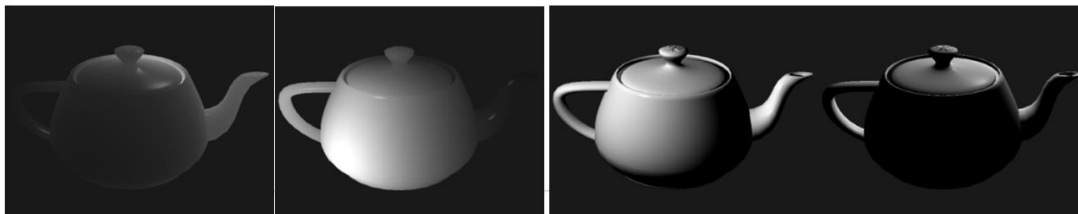


**Figure 3. Diffusion rendering (left) and BRDF rendering(right) where the parameters are  $\sigma_a = \{0.000103, 0.000097, 0.000100\}$ ,  $\sigma'_s = \{2.592, 2.592, 2.592\}$ ,  $\eta = 1.3352$**

Our rendering approach can simulate subsurface scattering effects in real-time but is limited by the constraint that the distance from the light to the object must remain constant. Using this rendering model, we simulated the skin parameters. The results of his simulation are illustrated in Figure 4. We can confirm that the color gets darker with a higher level of melanin and redder with a higher level of hemoglobin.

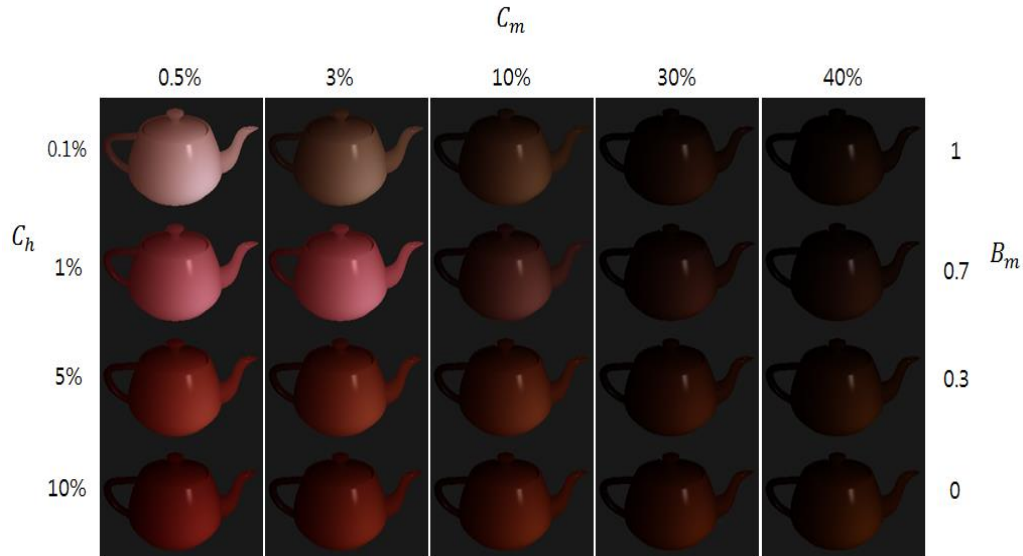


**Figure 4. Diffusion approximation simulation results obtained using extracted parameters**

#### 4.4. BRDF rendering

BRDF rendering is less complex than BSSRDF for two reasons. First, since we do not need to compute the distance  $r$ , the BRDF technique does not require a specialized rendering scheme. Second, as the total diffuse reflectance can be computed in a single evaluation of an equation, we do not need to compute  $R_d$  iteratively. Therefore, BRDF has higher computational efficiency, yet shows lower effectiveness in simulating subsurface scattering. The right-hand side image in Figure 4 shows the simulation result of BRDF rendering with our parameters, and Table 2 outlines the total diffuse reflectance computed by plugging the parameters into Eq. (9).

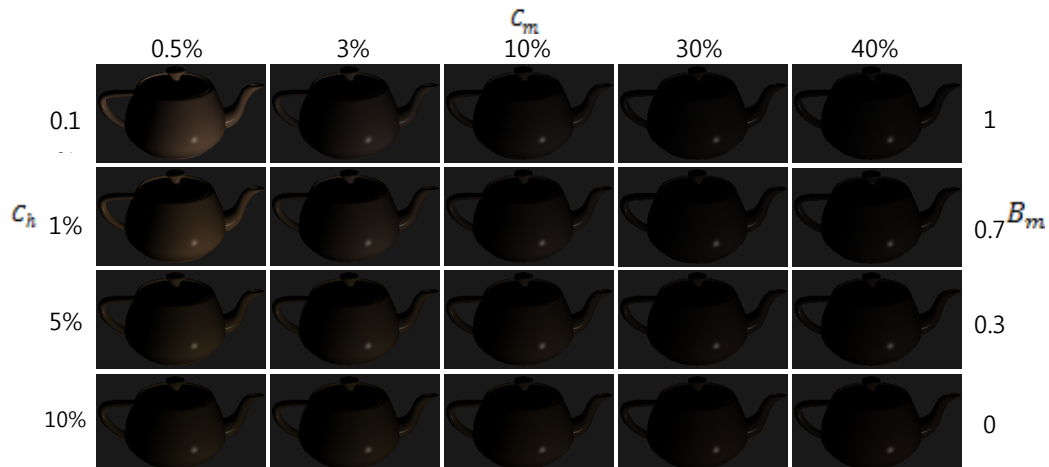


**Figure 5. BRDF approximation simulation results with the extracted parameters**

**Table 2. Total diffuse reflectance with different parameters for BRDF equation**

R	0.3016	0.1542	0.0951	0.0605	0.0537
G	0.2319	0.1258	0.0792	0.0509	0.0452
B	0.1795	0.1092	0.0709	0.0462	0.0412
R	0.2566	0.1577	0.1018	0.0658	0.0585
G	0.1937	0.1250	0.0821	0.0536	0.0477
B	0.1289	0.0981	0.0693	0.0467	0.0418
R	0.1643	0.1387	0.1055	0.0737	0.0663
G	0.1295	0.1080	0.0813	0.0565	0.0508
B	0.0785	0.0717	0.0598	0.0449	0.0409
R	0.1276	0.1197	0.1035	0.0803	0.0737
G	0.1023	0.0933	0.0777	0.0580	0.0529
B	0.0608	0.0580	0.0520	0.0422	0.0392

## 5. Conclusion

A spectrophotometer not only extracts the color of all objects in the CIE L\*a\*b space but also measures the spectral reflectance index. By comparing the extracted color and the  $C_m$ ,  $B_m$ , and  $C_h$  values suggested by Craig Donner using the data related to each value, we obtained the highest approximate values of  $C_m$ ,  $B_m$  and  $C_h$  for given melanin and hemoglobin levels. With the thus-obtained values, we computed the absorption and reduced scattering coefficients and further applied them to the dipole equation for rendering. As a spectrophotometer extracts both the color and reflection index of an object, we obtained the results for all the characteristics of the object itself. We plan to use a spectrophotometer to study the characteristics of not only the skin but also an object in the same manner as that used for extracting the absorption and scattering coefficients with a spectrophotometer.

## Acknowledgements

This research was partially funded by Korea Evaluation Institute of Industrial Technology, KEIT (Physically-based Cinematic Material Rendering Techniques optimized for Gameplay, No-10043453) and by Korea Science and Engineering Foundation (NRF) grant funded by the Korean government (2013 Super-realistic face modeling using parameterization of wound and scar).

## References

- [1] S. L. Jacques and D. J. McAuliffe, "The melanosome: threshold temperature for explosive vaporization and internal absorption coefficient during pulsed laser irradiation", *Photochemistry and photobiology*, vol. 53, no. 6, (1991), pp. 769, PubMed PMID: 1886936, ISSN: 0031-8655.
- [2] S. T. and H. A. Swartz. "The physical properties of melanins", *The Pigmentary System: Physiology and Pathophysiology*, Second Edition, (1998), pp. 311-341, Doi : 10.1002/9780470987100.ch16.
- [3] S. L. Jacques, "Skin optics", *Oregon Medical Laser Center News*, vol. 1998, no. 1, (1998), pp. 1-9, PubMed PMID: 2606488, <http://omlc.ogi.edu/news/jan98/skinoptics.html>.
- [4] H. W. Jensen, S. R. Marschner, M. Levoy and P. Hanrahan, "A practical model for subsurface light transport", *Proceedings of the 28th annual conference on Computer graphics and interactive techniques*, ACM, (2001), Doi: 10.1145/383259.383319.



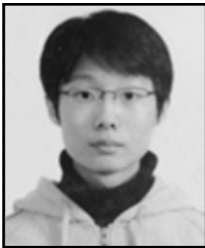
- [5] R. R. Anderson and J. A. Parrish, "The optics of human skin", *Journal of Investigative Dermatology*, vol. 77, no. 1, (1981), pp. 13-19, DOI: 10.1111/1523-1747.ep12479191.
- [6] D. Craig and H. W. Jensen, "A spectral BSSRDF for shading human skin", *Proceedings of the 17th Eurographics conference on Rendering Techniques. Eurographics Association*, (2006), Doi: 10.2312/EGWR/EGSR06/409-417.
- [7] T. Spott, L. O. Svaasand, R. E. Anderson and P. F. Schmedding, "Application of optical diffusion theory to transcutaneous bilirubinometry", In: *BiOS Europe'9, International Society for Optics and Photonics*, (1998), pp. 234-245, DOI: 10.1117/12.297907.
- [8] Z. George, J. Bykowski and N. Kollias "Skin melanin, hemoglobin, and light scattering properties can be quantitatively assessed in vivo using diffuse reflectance spectroscopy", *Journal of Investigative Dermatology*, vol. 117, no. 6, (2001), pp. 1452-1457, DOI: 10.1046/j.0022-202x.2001.01577.x.
- [9] A. N. Bashkatov, E. A. Genina, V. I. Kochubey and V. V. Tuchin, "Optical properties of human skin, subcutaneous and mucous tissues in the wavelength range from 400 to 2000 nm", *Journal of Physics D: Applied Physics*, vol. 38, no. 15, (2005), pp. 2543, DOI: 10.1088/0022-3727/38/15/004.
- [10] R. Wang, E. C.-Postava, D. Luebke, Q. Chen, W. Hua, Q. Peng and H. Bao, "Real-time editing and relighting of homogeneous translucent materials", *The Visual Computer*, vol. 24, no. 7-9, (2008), pp. 565-575, DOI: 10.1007/s00371-008-0237-9.
- [11] M. A. Shah, J. Kontinen and S. Pattanaik, "Image-Space Subsurface Scattering for Interactive Rendering of Deformable Translucent Objects", *IEEE Computer Society*, (2009), pp. 66-78, DOI: 10.1109/MCG.2009.11.
- [12] S. Moon, S. Lee, S. Kim, H. Hyun and S. Chin, "Cinematic Wound Synthesis Optimized for Real-time Gameplay".
- [13] R. Ponalagusamy and R. T. Selvi, "Blood Flow through Stenosed Arteries: New Formula for Computing Peripheral Plasma Layer Thickness", *International Journal of Bio-Science and Bio-Technology*, vol. 3, no. 1, (2011), pp. 27-38, ISSN: 2233-7849.
- [14] S. G. Babiker, Y. Shuai, M. O. Sid-Ahmed, M. Xie and M. Liu, "Enhancement of Optical Absorption in an Amorphous Silicon Solar Cell with Periodic Grating Structure", DOI: 10.1063/1.3569689.

## Authors



**Seonghyun Moon**

He is a research associate at XICOM (visual and virtual reality computing) Lab in Sungkyul University, South Korea. His research interests include game programming, sub-surface scattering and geometry modeling. He actively participates in working at research projects related to tasks on super-realistic wound synthesis on a 3d face and cinematic rendering techniques.



**Seonghee Lee**

He is an undergraduate course student in Department of Multimedia Engineering, Sungkyul University in South Korea. He is a member of XICOM (visual and virtual reality computing) Lab. His research interests include shader programming and sub-surface scattering and real-time rendering. He also participates in enhancing of material rendering tasks in real-time.



### **Seongah Chin**

He is a professor and director of XICOM Lab at the Division of Multimedia Engineering in the College of Engineering in Sungkyul University, South Korea. His primary research interests include visual computing, virtual reality, computer vision and brain computer interface. He has published research papers into international journals including IEEE Transactions on SMC-C, IEEE Transactions on CE, AI-EDAM, Chinese Optics Letters, Computers in Industry, Color Research and Application, and Computer Animation and Virtual Worlds and so on. He has actively served lots of international conferences on his primary research fields as program committees. He has received research grants mostly from Korea government including NRF, KEIT, KSF, KRF, KOSEF, and SMBA etc. as well. Before joining SKU in 2001, he was a research professor at department of digital media technology in Sogang University. Also he spent his sabbatical year as a visiting research professor at IME department in Wayne State University in USA in 2007. Dr. Chin received his PhD in Computer Science from the Steven Institute of Technology in Hoboken, New Jersey, in 1999. He also received his BS and MS degrees in Mathematics and Computer Science from Chonbuk National University, in Chonju, South Korea, in 1991 and 1993, respectively.